

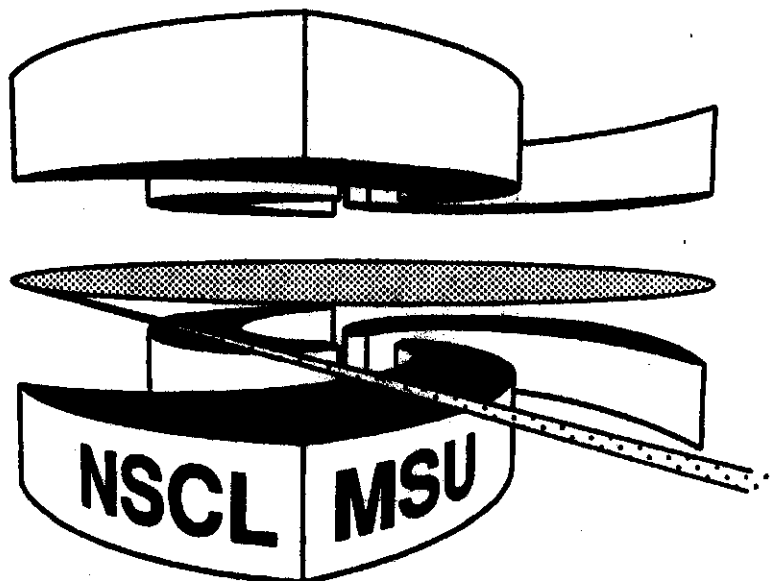


Michigan State University

National Superconducting Cyclotron Laboratory

**FAST-FOURIER-TURNFORM SPECTRAL ENHANCEMENT
TECHNIQUES FOR γ -RAY SPECTROSCOPY**

C.V. HAMPTON, B. LIAN, and WM. C. McHARRIS



Fast-Fourier-Transform Spectral Enhancement Techniques for γ -Ray Spectroscopy

C. V. Hampton, B. Lian, and Wm. C. McHarris

National Superconducting Cyclotron Laboratory and Departments of Chemistry and Physics/Astronomy, Michigan State University, East Lansing MI 48824

The application of a discrete, Fast-Fourier-Transformation algorithm to multiply-gated γ -ray spectra enhances low intensity components, removes high-frequency noise, and increases the signal-to-background ratio. This method is preferable to a three-point smoothing technique for low- and medium-intensity peaks.

1. Introduction

About twenty years ago, spectroscopists used a form of Fourier transform (FT) for γ -ray spectroscopy, with some success. Some built the continuous FT algorithm into a smoothing technique, using a math filter that operated on the transformed coefficient vector [1-4]. Others constructed a deconvolution technique based on the Fourier transform [5-7]. These were designed specifically for each data set. Both methods improved spectral quality; however, the computer software and hardware of the time may have prevented the routine use of a fast-fourier-transform (FFT). Inouye [1] in 1969, using the continuous FT, speculated that a transform of a 4096-channel spectrum might require about 1/2 hour of computer time, and Blinowska and Wessner [2] in 1974 reported that a FFT of a 1024-channel spectrum required 50 seconds. Today, the forward and reverse FFT's are virtually instantaneous on a system such as Dec's VAXstation 4000.

With the advent of 4π spectrometers and the search for low intensity, superdeformed bands in nuclear structure studies, the need for FFT again arises. Even though the γ -ray signal-to-noise ratio from a single detector may be adequate, multistep coincidence measurements among various detectors produce large amounts of white noise within the resulting spectrum. High frequency noise is systematically introduced through the analysis process, especially the process of rebinning doppler- and gain-shifted data via a random number sequence. When this is compounded with the necessity of investigating peaks below the 10% intensity level, the need for a potent noise reduction method becomes very apparent.

A data set obtained from the ^{37}Cl on ^{100}Mo reaction [8], using the 21-detector array at Holifield (Oak Ridge National Laboratory), provided a unique opportunity for this technique development. For example, most of the peaks of interest in the rotational band structure of one of the prime product nuclei of interest, the odd-odd ^{132}Pr nucleus, are below the 20% count level, and peaks associated with its superdeformed bands have considerably lower intensities, lower by more than an order of magnitude.

2. Software

The Oak Ridge User Software was modified to accommodate a discrete FFT program from the IMSL package [9], which uses a variation of the Cooley-Tukey algorithm [10]. The discrete Fast Fourier Transform of a vector of size N is most efficient when using a fixed number of points based on a product of small prime numbers. If this condition is met, then the computation is proportional to $N \log N$; otherwise, the number of computational operations is equal to N^2 . The real, trigonometric FFT that is used is related to the continuous Fourier transform [11], defined as

$$\hat{f}(\omega) = \int_{-\infty}^{+\infty} f(t)e^{-2\pi i\omega t} dt. \quad (1)$$

The discrete FFT uses an approximation of this integral and accepts a vector \vec{f} of length N , then returns a coefficient vector \vec{c} with the following form (if N is even)

$$\vec{c}_{2m-2} = + \sum_{n=1}^N \vec{f}_n \cos \left[\frac{(m-1)(n-1)2\pi}{N} \right] \quad m = 2, \dots, N/2 + 1 \quad (2)$$

$$\bar{c}_{2m-1} = - \sum_{n=1}^N \bar{s}_n \sin \left[\frac{(m-1)(n-1)2\pi}{N} \right] \quad m = 2, \dots, N/2$$

$$\bar{c}_1 = + \sum_{n=1}^N \bar{s}_n.$$

If N is odd, \bar{c}_m is defined as above for m ranging from 2 to $(N+1)/2$. The spectra \bar{s}_m are transformed into another domain, \bar{c} , which may be thought of as a frequency domain. Then a limited range of frequencies —excluding the highest frequencies — are chosen to be transformed back into the original domain. Fig. 1 shows the direct equivalence between frequency of the forward FFT and the channel number of the data. Because of this, the range for the reverse FFT can be set according to channel number. There is no mathematical manipulation of the forward transform, making the technique simple to use. To initialize the program, only the forward and reverse channel-number ranges need to be specified, along with input and output math operators. This constitutes the entire noise reduction technique.

3. Algorithm Development

There were three mathematical considerations that had to be built into the algorithm in order to produce an acceptable transformed spectrum.

A. Zero Suppression

Gated spectra often contain zero points in the baseline due to the position of the gate. This constitutes a non-continuous function, and the FFT produced has a ringing pattern superimposed on the spectrum. To resolve this, the zero points were removed, their channel number positions were retained, and the spectrum was compressed (shifted). After the reverse FFT, the spectrum was reconstructed with the zero points in place.

B. Baseline Offset

An offset is added to the spectrum before FFT to avoid an arithmetic error in the math operator if a negative value is present. The offset is subtracted after the reverse FFT.

C. Mathematical Operator

If the data set intensities vary over many orders of magnitude, a linear FFT algorithm will be useful for only a portion of the data set. A series of math operators were included in order to extend the range. The software was written so that the user has a choice of math operators and each data set can be individually optimized. The common and natural log operators can work over a few orders of magnitude; the square root operator selectively enhances the small peaks (noise) for a very efficient removal of noise. By using a combination of operators, the best results, covering over eight orders of magnitude, are obtained. Taking the square root, then using the ln operator twice (LLS), yields the best results if a large, multiple spectra, data set is to be analyzed at one time. It is also possible to vary the input operator for the forward transform with respect to the output operator for the reverse transform. For example, a combination of \ln/\log^{-1} provides extra enhancement for the low intensity peaks. These techniques must be used selectively; there are advantages and disadvantages to both the LLS and \ln/\log^{-1} methods. LLS can be used for multiple calls to the FFT routine on a data set with widely varying intensities. Using LLS twice on the same data set is preferable to using a high percentage of noise reduction in a single attempt. LLS can be used on data that have been background subtracted or baselined with the SNIP routine (see below). The \ln/\log^{-1} method is for single use only on individual spectra. It maximizes low intensity peaks and minimizes background. However,

it must be performed before background subtraction, since negative peaks are transformed into positive peaks, and it must be used before SNIP baseline subtraction if the relative peak ratios are to be retained.

4. Baseline Spectrum

In order to generate the baseline or low-frequency component of the spectrum, another routine was added to the Oak Ridge software — a modification of the Statistics-Sensitive Nonlinear Iterative Peak clipping (SNIP) algorithm that was developed for proton-induced x-ray emission spectroscopy [12].

Both SNIP and FFT routines require the same mathematical treatment for zero suppression of the channel-number axis (X) and baseline offset of the intensity axis (Y) of the spectra. The LLS combination of math operators is optional in the FFT algorithm but a requirement in SNIP, since it is used as a low statistics filter to compress the Y-axis range. The channel number intensity can be represented as: $z = \mathcal{F}(y)$ where

$$\mathcal{F}(y) = \ln \left[\ln \left(\sqrt{y - [offset] + 1} + 1 \right) + 1 \right]. \quad (3)$$

After the FFT routine, but before the application of the reverse operator, a multipass peak clipping loop replaces each value of $z(x)$. For each pass of the loop, a sampling interval ω is named. The average of the counts at each end of the sampling interval, $\bar{z}(x, \omega)$, is compared with the intensity at the center of the interval, $z(x)$, and the minimum value, $\bar{z}[x, \omega(x)]$, is written as the new channel count:

$$\left\{ \begin{array}{l} \bar{z}(x, \omega) = [z(x + \omega) + z(x - \omega)]/2 \\ z(x) \end{array} \right\} \begin{array}{l} \text{MIN} \\ \Rightarrow \\ \text{(MAX)} \end{array} \bar{z}[x, \omega(x)]. \quad (4)$$

After each pass, the sampling interval is incremented by 1 to reduce baseline oscillations; on the next to the last pass, the interval is reset to 1. The process is repeated for each channel.

A provision is made for low intensity spectra (≤ 500 counts) to insure a realistic baseline that places negative peaks properly. For the first two passes through the loop, the maximum value of $z(x)$ and $\bar{z}(x, \omega)$ is averaged with the minimum value. The low-intensity spectra are subjected to twenty seven passes through the loop, whereas higher intensity spectra use nine loop passes. The reverse operator changes the results back to channel counts. Resulting baseline spectra generated by SNIP for low- and high-intensity conditions are shown in Fig. 2, along with their corresponding energy spectra.

5. Comparison with a Smoothing Technique

A resolution study was performed to determine what effect FFT and a box-car averaging or smoothing technique had on the full-width at half-maximum peak measurement (FWHM). Three single-channel gates with the intensity ratio 1: 2.3: 5.9 were chosen since they all contain a peak at 283 keV. The FWHM results for this peak in each data set are listed in Table 1. The original data are compared with the FFT (LLS) data, a three-point smooth, and a five-point smooth of the data. The resolution listed are given in keV ($\approx \pm 0.05$). There is no change in the resolution between the original data and the three-point smooth for medium- and high- intensity gates. However, there is a significant decrease in the resolution of the peak between the original and the three-point smoothed data from the low-intensity gate. The resolution of all three gates decreased using the five-point smooth, whereas the resolution of all three apparently increased after using FFT. A direct comparison of the effect of FFT and smoothing on a large part of the spectrum is shown in Fig. 3: A) shows the original, low-intensity, single gate at channel 174. B) shows the first FFT (LLS) on the original data. FFT can be performed any number of times on the same data in a successive manner. C) shows the second FFT (\ln/\log^{-1}) in succession. Compare these results with those from the averaging techniques: D) shows a three-point and E) a five-point smooth on the original data.

6. Summary

The Oak Ridge Holifield Nuclear Spectroscopy User Software has been modified to include FFT and SNIP spectral enhancement routines for both single and multiple spectra, using their command file (cmd) structure. This work shows that the application of a discrete FFT algorithm to multiply-gated γ -ray spectra enhances low-intensity components, removes high-frequency noise, and increases the signal-to-background ratio. The method is extremely fast and uncomplicated; only a channel-number range and a math operator need to be specified. It is preferable to a three-point smoothing technique. Peaks beneath noise level can actually be seen once the noise frequencies have been removed. The technique is most beneficial for low- and medium-intensity gated spectra. As an added bonus, FFT appears to increase the resolution of the peaks. The next step in the continuation of this work will be a two-dimensional FFT of the $E_{\gamma 1}$ versus $E_{\gamma 2}$ data array.

Table 1. FFT versus Smoothing: Resolution comparison for low- (174), medium- (179) and high-intensity (202) single-channel gates. The resolution (FWHM) of the 283 keV. peak from each gate is listed in keV.

	Channel-174 gate (Low)	Channel-179 gate (Medium)	Channel-202 gate (High)
Original data	2.49	2.49	2.49
FFT (LLS)	1.87	1.87	1.87
3-point smooth	3.42	2.49	2.49
5-point smooth	4.36	3.11	3.74

1. T. Inouye, T. Harper, N.C. Rasmussen, Nucl. Instr. Meth., 67 (1969) 125.
2. K.J. Blinowska, E.F. Wessner, Nucl. Instr. Meth., 118 (1974) 597.
3. H.B. Kekre, V.K. Madan, Nucl. Instr. Meth., A245 (1986) 542.
4. H.B. Kekre, V.K. Madan, B.R. Bairi, Nucl. Instr. Meth., A279 (1989) 596.
5. R. Verma, Nucl. Instr. Meth., 212 (1983) 323.
6. A. Cabral-Prieto, H. Jimenez-Dominguez, M. Torres-Valderrama, Nucl. Instr. Meth., B54 (1991) 532.
7. H. Flores-Llamas, H. Yee-Madeira, Nucl. Instr. Meth., B71 (1992) 103.
8. C.V. Hampton, Aracelys Rios, W.A. Olivier, R.M. Ronningen, Wm. C. McHarris, and ORNL Nuclear Structure Research Group, "Superdeformation in Odd-Odd ^{132}Pr ", NSCL Annual Report, Michigan State University (1991), p29.
9. IMSL, Inc., Math/Library Software. The algorithm used is based on the real trigonometric FFT developed by Paul Swartrauber at the National Center for Atmospheric Research.
10. J.W. Cooley, and J.W. Tukey, *Mathematics of Computation*, 19, (1965), 297.
11. E. Oran Brigham, *The Fast Fourier Transform*, Prentice-Hall, Englewood Cliffs, N.J. (1974).
12. C.G. Ryan, E. Clayton, W.L. Griffin, S.H. Sie, D.R. Consens, Nucl. Instr. Meth., B34 (1988) 396.

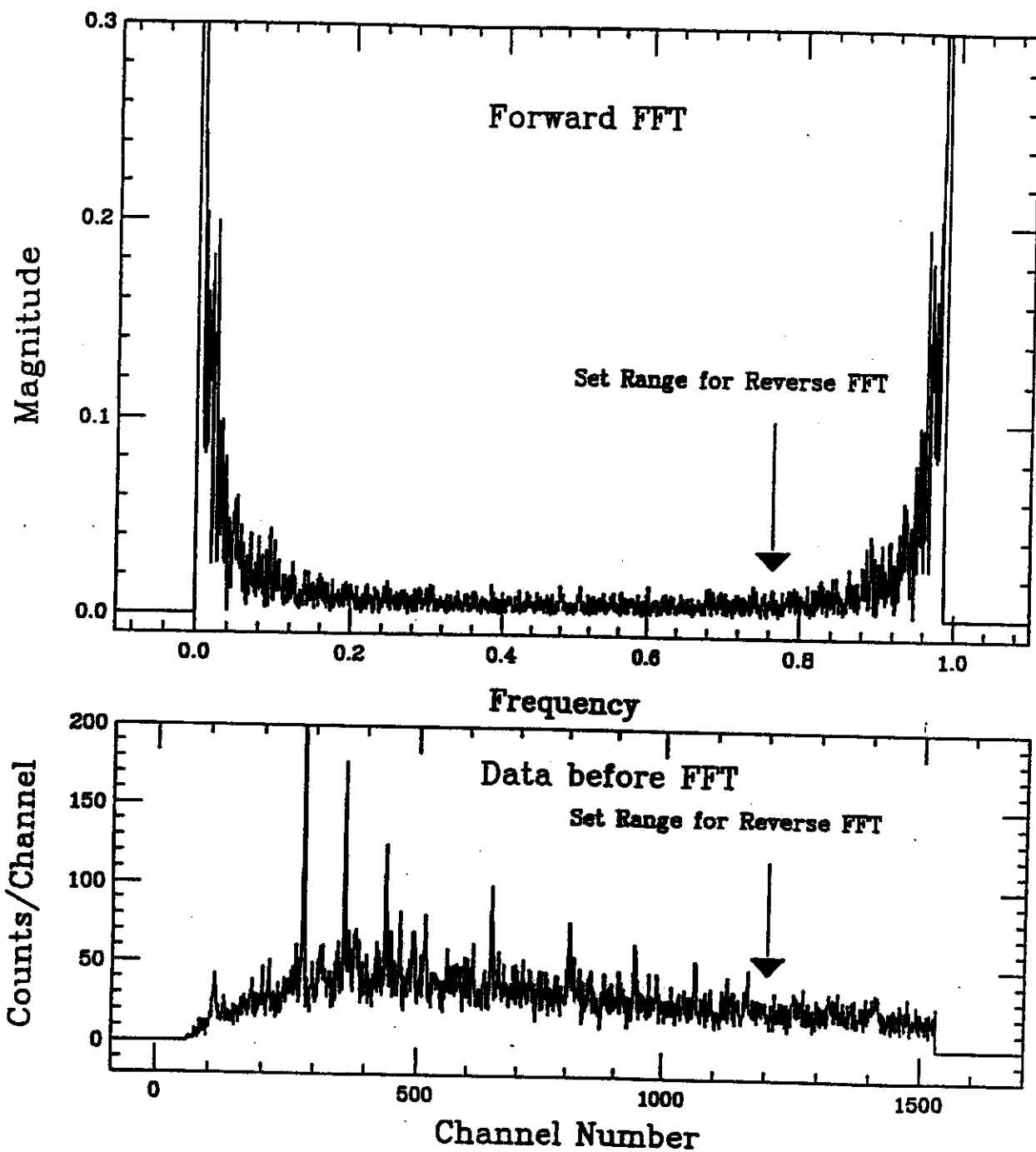


Fig. 1. Equivalence between FFT frequency and spectral channel number: A plot of a forward FFT (linear) of a 240 keV gate. Since there is a direct relationship between points on the frequency axis and on the channel number axis, setting the range for the reverse FFT is based on channel number.

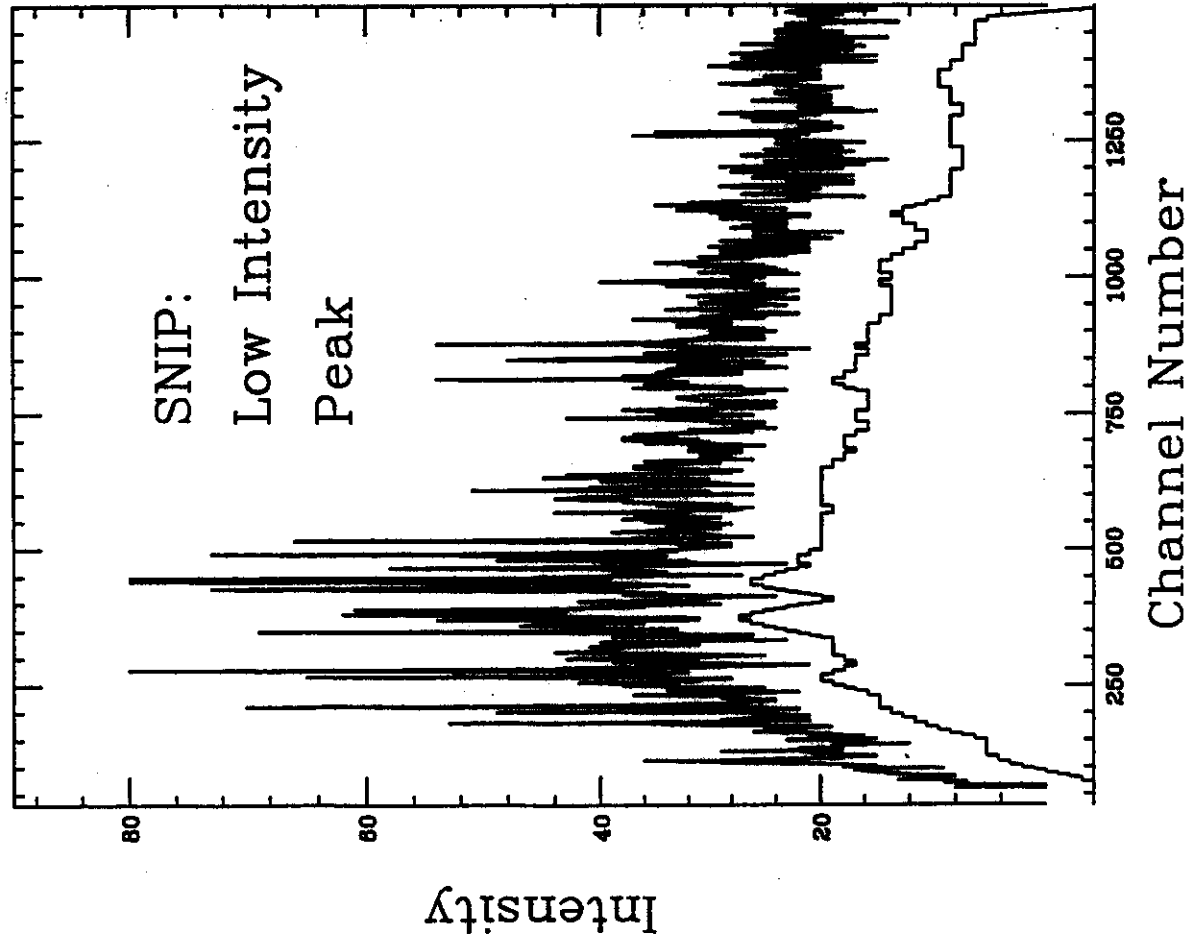
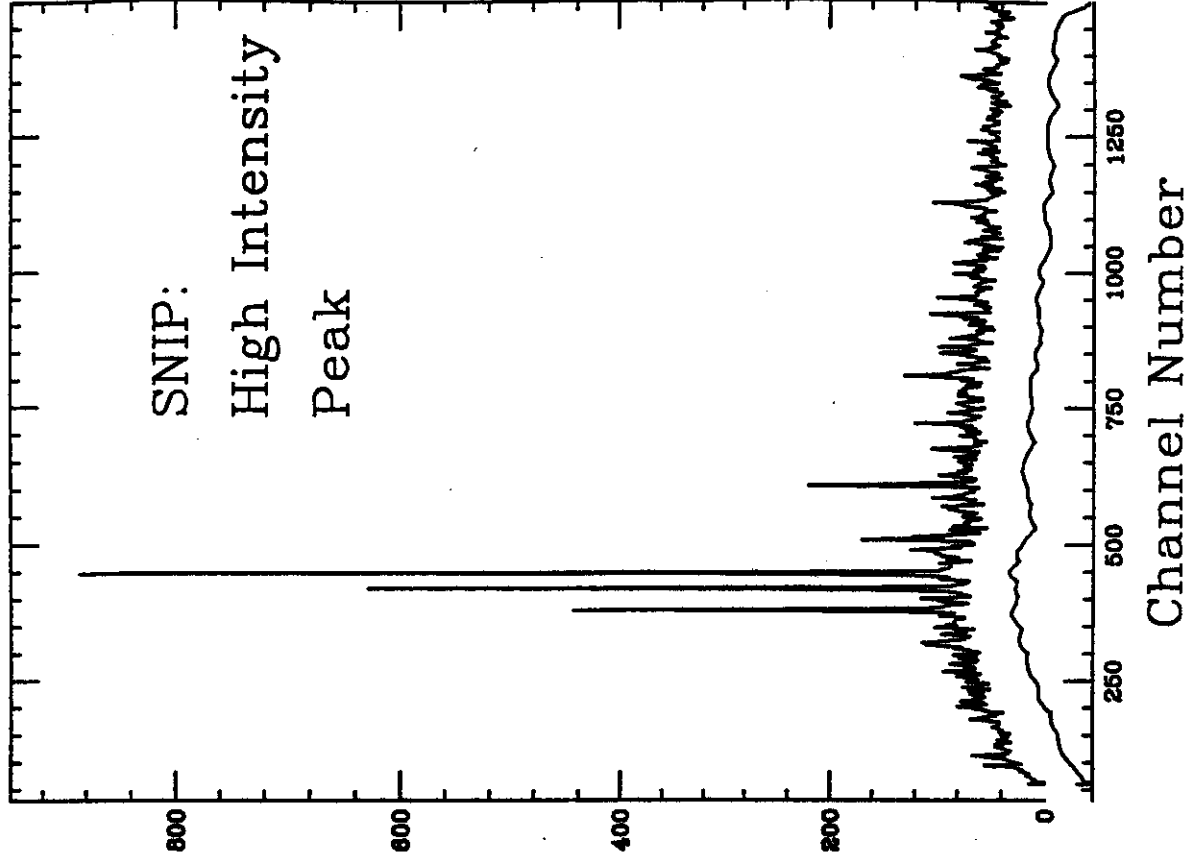


Fig. 2. SNIP baseline generation for low- and high-intensity peaks.

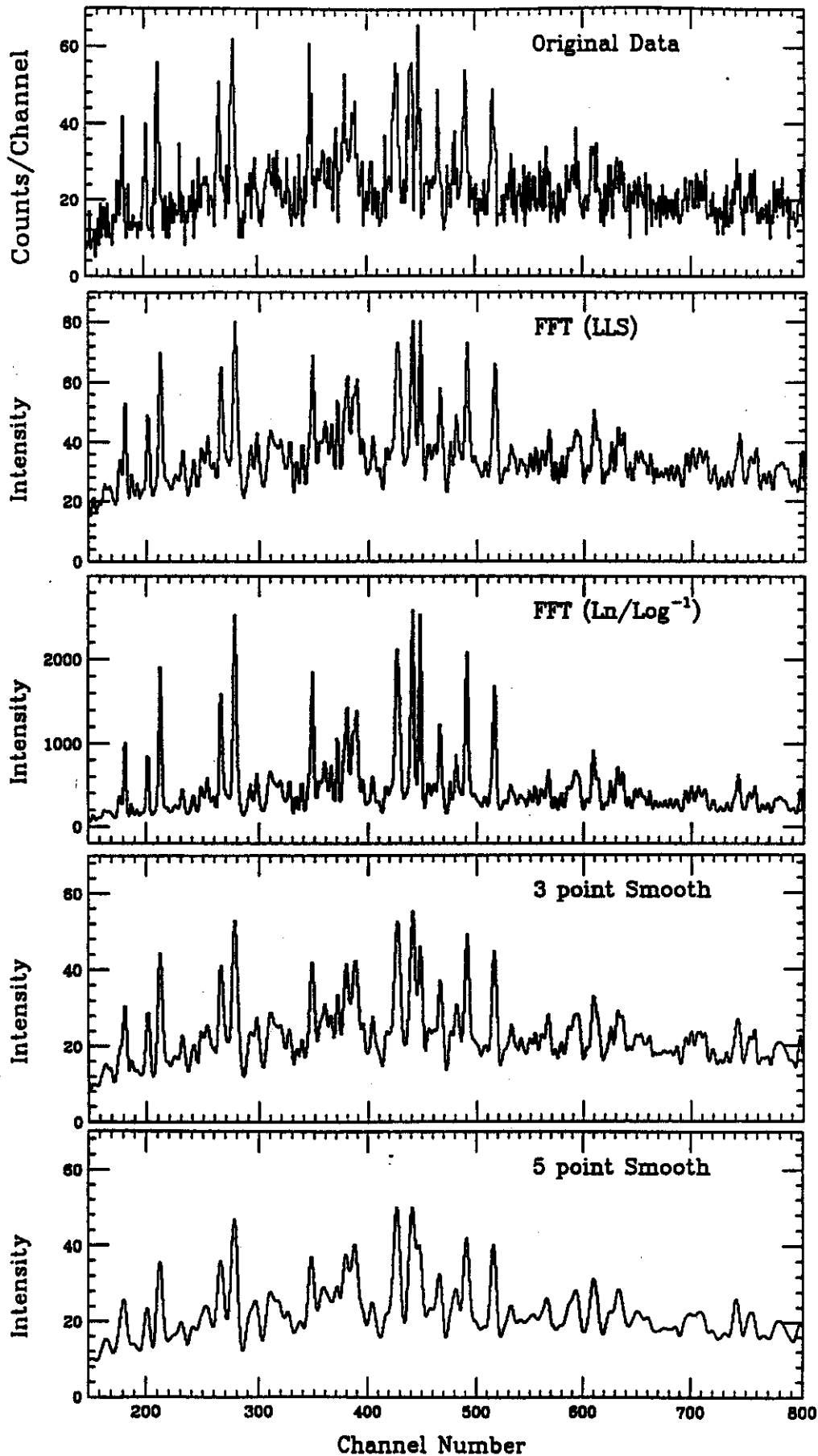


Fig. 3. A) Original, single gate at channel 174. B) First FFT (LLS) on original data. C) Second FFT (\ln/\log^{-1}). D) Three point smooth on original data. E) Five point smooth on original data.